Article

Not peer-reviewed version

Novel Intravitreal Retina-Targeting and Immune-Evading Adeno-Associated Virus Capsid Variant

Zhongshan Cai , Yawen Liu , Li Zhao , Xiaofang Li , Binwu Zhang , Yuxu Tang , Tao Zhou , Zhuxia Zheng , Aonan Li , Jiye Wei , Qingzhou Ji * , Daru Lu * , Damien Marsic *

Posted Date: 27 September 2024

doi: 10.20944/preprints202409.2179.v1

Keywords: AAV; capsid; intravitreal; retina; immune evasion

 doi:10.20944/preprints202409.2179.v

Article

Novel Intravitreal Retina-Targeting and Immune-Evading Adeno-Associated Virus Capsid Variant

Zhongshan Cai [1,2], Yawen Liu [2], Li Zhao [2], Xiaofang Li [2], Binwu Zhang [2], Yuxu Tang [2], Tao Zhou [3], Zhuxia Zheng [3], Aonan Li [3], Jiye Wei [3], Qingzhou Ji [2,*], Daru Lu [1,*] and Damien Marsic [2,4,*]

[1] MOE Engineering Research Center of Gene Technology , Obstetrics and Gynecology Hospital, Fudan University, Shanghai, China
[2] Porton Advanced Solutions, 388 Xinping St, Suzhou Industrial Park, Jiangsu, China
[3] ViewGene Therapeutics, 1 Hua Yun Rd, Suzhou Industrial Park, Jiangsu, China
[4] MaiBo Biotech, 1 Hanlin Rd, Suzhou Industrial Park, Jiangsu
* Correspondence: qingzhou.ji@portonadvanced.com (Q.J.); drlu@fudan.edu.cn (D.L.); damien.marsic@maibo-biotech.com (D.M.)

Abstract: Retinal diseases are an important focus of in vivo gene therapy, for which adeno-associated virus is a preferred vector. Intravitreal injection is a highly desirable delivery route because it is much simpler, safer and inexpensive than the main alternative subretinal injection. However, existing capsids have low efficiency, require high doses and are susceptible to neutralization by antibodies that are present in the vitreous. Using AAV5 as starting material, we applied a combination of directed evolution and rational design to develop PT1, a novel AAV capsid capable of efficiently transducing the retina after intravitreal injection. The most striking property of PT1 is its remarkable ability to evade preexisting neutralizing antibodies, thanks to its multiple mutations spread over large areas of the capsid surface, disrupting several epitopes. Our results suggest that PT1 has a strong potential as a useful candidate capsid for human retinal gene therapy.

Keywords: AAV; capsid; intravitreal; retina; immune evasion

1. Introduction

Adeno-associated virus (AAV) has emerged as the viral vector of choice for human in vivo gene therapy in both clinical trials and approved therapies. To date, 29 in vivo gene therapies have been approved by some regulatory agency (mostly the FDA). Of these, 12 use a viral vector, including 7 using an AAV [1]. The eye, and more specifically the retina, is a particularly important target for gene therapy, representing 23% of all AAV-mediated clinical trials [2]. A search on clinicaltrials.gov showed 92 trials targeting the retina out of 100 eye-directed AAV-mediated clinical trials. Luxturna, which uses a wild type AAV2 capsid, is the only approved retinal gene therapy so far [3]. It is delivered by subretinal injection, a complex and risky surgical procedure requiring hospitalization. The main alternative to subretinal delivery is intravitreal injection, which is a simple, safe and cheap procedure than can be performed by a nurse in an office setting. The reason why subretinal injection has been favored (54 clinical trials vs 32 for intravitreal injection) is that it's much more efficient. Very few capsid serotypes are capable of transducing the retina when injected intravitreally, and those require large doses (typically 2 orders of magnitude more than via the subretinal route) to compensate for the lower efficiency. In addition, while the subretinal space is immune privileged, the vitreous contains potentially neutralizing antibodies [4], requiring patients to be screened and eventually excluded from receiving the gene therapy if they have high titers of antibodies neutralizing the capsid being used. On the other hand, intravitreal injection has the notable advantage of targeting a larger area of the retina, while the viral vectors injected subretinally tend to transduce a small area at the injection location.

As there is no selective pressure in nature to evolve capsids into efficient gene therapy vectors, efforts have been made during the past 2 decades to develop engineered capsids with improved properties, using a range of approaches including directed evolution, rational design or a combination

 doi:10.20944/preprints202409.2179.v

of both [1,5,6]. The property that attracted most attention is the ability to efficiently target specific tissues or cell populations via a particular administration route, by modifying the capsid surface to disrupt or promote interactions with cell surface receptors [7–9]. Another important property is transduction efficiency, which can be improved independently of tissue specificity, by enhancing the capsid's ability to evade degradation after cell entry [10]. Not much efforts have been put, in the field of retinal gene therapy, into developing capsids able to evade preexisting neutralizing antibodies, with the property emerging just as a side effect of introducing surface mutations in an effort to alter tropism [9]. Finally, another property that can be affected by capsid engineering is the efficiency of capsid assembly. Unlike with other properties, capsid engineering is unlikely to improve what has already been optimized by natural selection; on the contrary, each alteration of the capsid amino acid sequence risks adversely affecting the ability of the monomers to fold correctly and assemble into a functioning capsid, resulting in a lower AAV production yield. Considering the high costs of producing AAV, novel engineered capsids with enhanced tissue specificity or transduction efficiency therefore also need to be evaluated for the ability to produce AAV with a reasonable yield.

Progress has been incremental so far, and much more work is needed in order to make ocular gene therapy more accessible. The development of novel AAV capsids capable of more efficienctly transduce retinal tissue after intravitreal injection while successfully evading preexisting neutralizing antibodies will make retinal gene therapy safer, cheaper and accessible to larger patient populations.

Here we introduce a new AAV capsid variant resulting from a combination of incremental directed evolution and rational design, with a large number of mutations across wide areas of the capsid surface, capable of penetrating deep into the various retina layers and with a remarkable ability to evade preexisting neutralizing antibodies.

2. Results

2.1. Capsid Variant Development

An AAV5-based capsid library was developed as previously described [11,12] and subjected to 2 rounds of in vivo selection in NHP retina via intravitreal injection. An enriched capsid variant with a total of 8 amino acid substitutions in 3 variable regions was identified: TEN to EKH at 376-378 in VR-III, S518K in VR-VI, and ND to SE at 694-695, Q697T and T706A in VR-IX (Figure 1). A new capsid library was then designed and constructed based on that variant, with mutations in variable regions IV and VIII. The new library was subjected to a single round of in vivo selection in murine retina via intravitreal injection. Enriched mutation N443A (VR-IV) as well as enriched motif consisting of mutations N573A, SST to NAS at 575-577 and AT to TA at 581-582 (VR-VIII) were identified. Finally, as we had previously observed in swapping experiments that the transduction efficiency of AAV5-derived capsid variants can be significantly increased by replacing their VP1-unique region by that of AAV8 (unpublished), it was decided to apply this sequence swap to our new variant. In summary, the final capsid variant, referred to hereafter as PT1, can be defined, as illustrated in Figure 1, as having an AAV8 VP1-unique region, with the rest of the sequence deriving from AAV5 with a total of 15 amino acid substitutions in 5 different variable regions.

 doi:10.20944/preprints202409.2179.v1

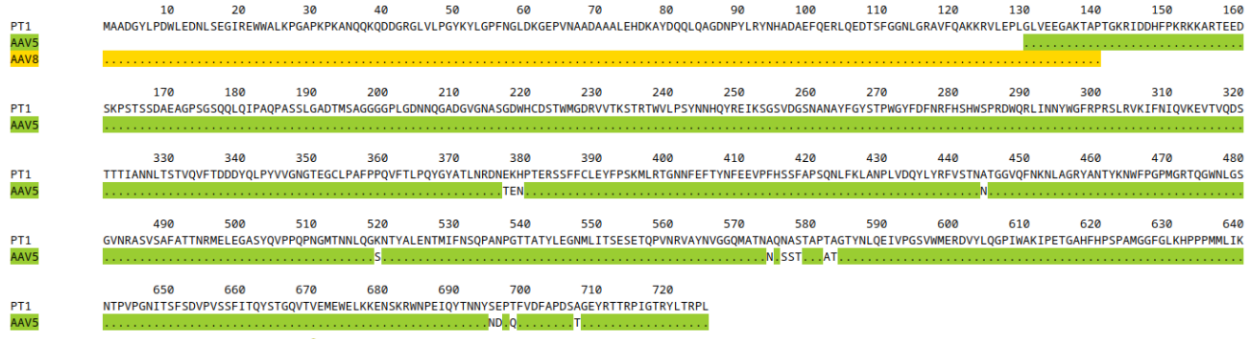

Variant region	Parent / feature	Parent region	Variant sequence	Parent sequence	Variable region	Selected in
1-140	AAV8	1-140				In vitro
130-376	AAV5	129-375				
377-379	substitution	376-378	EKH	TEN	III	NHP
380-443	AAV5	379-442				
444	substitution	443	A	N	IV	Mouse
445-518	AAV5	444-517				
519	substitution	518	K	S	VI	NHP
520-573	AAV5	519-572				
574	substitution	573	A	N	VIII	Mouse
575	AAV5	574			VIII	
576-578	substitution	575-577	NAS	SST	VIII	Mouse
579-581	AAV5	578-580			VIII	
582-583	substitution	581-582	TA	AT	VIII	Mouse
584-694	AAV5	583-693				
695-696	substitution	694-695	SE	ND	IX	NHP
697	AAV5	696			IX	
698	substitution	697	T	Q	IX	NHP
699-706	AAV5	698-705			IX	
707	substitution	706	A	T	IX	NHP
708-725	AAV5	707-724				

Figure 1. Sequence features of capsid variant PT1. Top: amino acid sequence of PT1 capsid VP1 protein compared with parent capsids AV8 (gold) and AAV5 (green). Dots indicate identity. Parental sequences are only shown when they differ from that of PT1. Bottom left: Three-dimensional model of AAV5 capsid showing the surface substitutions of PT1 color coded according to their region (red: VR-III, green: VR-IV, blue: VR-VI, yellow: VR-VIII, magenta: VR-IX). Bottom right: detailed description of PT1 capsid VP1 sequence. Substitutions are color-coded in the same way as the model on the left.

 doi:10.20944/preprints202409.2179.v

2.2. Recombinant AAV Preparations

Four capsid variants capable of transducing retina after intravitreal injection were selected as controls to which the novel capsid PT1 was to be compared. Wild type AAV2, used in the first approved retinal gene therapy Luxturna (although administered subretinally) as well as in most early clinical trials of intravitreally injected gene therapies, was an obvious first choice. Two other AAV2-derived capsids with improved properties, the rationally designed quintuple mutant AAV2(quadY-F+T-V) [10], hereafter designated as quadYFTV, and the evolved capsid 7m8, harboring a 10 amino acid insertion in variable region VIII [7], were chosen as well. Finally, the recently described AAV5-derived LSV1 [13] seemed to be particularly relevant as being a capsid variant quite similar to PT1 but with a different set of mutations.

A recombinant AAV genome encoding GFP was packaged with the 5 capsid variants (PT1 and the 4 controls). Two preparations, 7m8 and quadYFTV, had high endotoxin levels and were subjected to an endotoxin removal step [14]. As expected, the AAV5-derived variants LSV1 and PT1 had higher yields (2.8E13 and 2.6E13 vg respectively) than the AAV2-derived capsids (7.2E12 to 1.5E13 vg). In order to reach the same working titer for all preparations, 4 of them were diluted to the same titer as AAV2, which was the lowest at 7.22E12 vg/ml.

2.3. In Vitro Transduction

Transduction efficiency of PT1 was compared to that of the 4 control capsids AAV2, quadYFTV, 7m8 and LSV1 in the relevant human retina-derived ARPE-19 [15] cell line. As shown in Figure 2 (left), all 5 capsids show similar transduction, from 79.8% GFP-positive cells for AAV2 to 91.6% for LSV1, with PT1 being in the middle at 86.8%.

In addition, transduction efficiencies of PT1 and AAV2 were compared in 5 additional human-derived cell lines: A549, HepG2, HuH-7, SKOV-3 and BxPC-3 (Figure 2 right). AAV2 appears to be quite promiscuous, with over 40% transduction in all 6 cell lines, lowest at 43.1% in A549 and highest in the 2 liver-derived cell lines HuH-7 (90.2%) and HepG2 (87.8%). In contrast, PT1 shows strong retinal specificity, with 86.8% transduction in ARPE-19, significantly lower in HuH-7 (62.6%) and much lower (below 40%) in all 4 other cell lines.

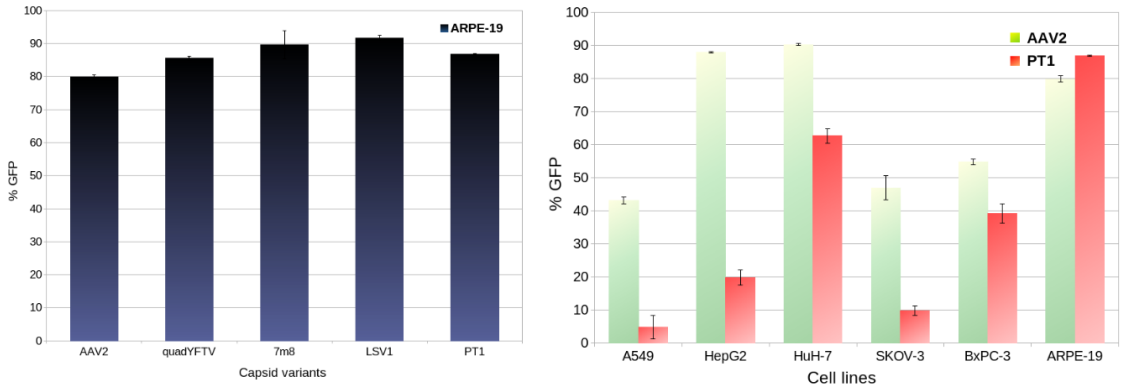

Figure 2. In vitro transduction comparisons. Left: transduction efficiencies (percentage of GFP-positive cells) in the ARPE-19 cell line of PT1 compared with that of 4 control capsids. Right: comparison of transduction efficiencies of AAV2 and PT1 in 6 different cell lines. Error bars show standard deviation.

2.4. Immune Evasion

In order to compare to what extent can PT1 evade preexisting neutralizing antibodies compared to the 4 control capsids, human retina-derived ARPE-19 cells preincubated with increasing amounts of commercial intravenous immunogobulin (IVIG) were infected with GFP-encoding rAAV preparations. Three days later, the prevalence of GFP-expressing cells was quantified by flow cytometry. As shown in Figure 3, while all 4 controls saw a 90% or more decrease in transduction at 100 µg/ml IVIG,

 doi:10.20944/preprints202409.2179.v

900 µg/ml IVIG were necessary to achieve the same level of neutralization with PT1. The IVIG concentration required to reach 50% neutralization was 14, 15, 21, 31 and 286 µg/ml respectively for AAV2, quadYFTV, 7m8, LSV1 and PT1.

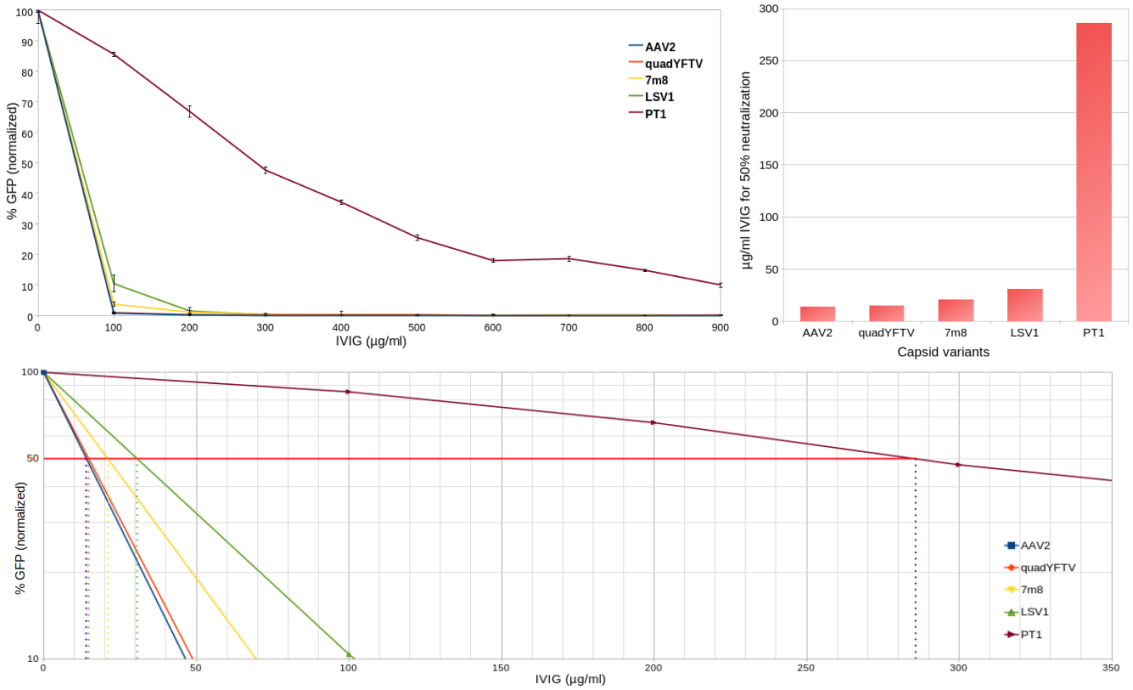

Figure 3. In vitro neutralization assays of PT1 and 4 control capsids in ARPE-19 cells. Top left: comparison of transduction neutralization by increasing amounts of IVIG of PT1 and 4 control capsids. Error bars represent standard deviation. Bottom: zoom of relevant area of above chart with Y-axis converted to logarithmic scale for easier visualization of the IVIG concentrations at which 50% neutralization is achieved. Top right: comparison of neutralization scores (IVIG concentration needed for 50% decrease in transduction) for PT1 and the 4 control capsids.

To assess whether PT1 would display similar immune evading properties under different experimental conditions, the neutralization assay was repeated using 5 additional human cell lines but with AAV2 only as a control (Figure 4). The same pattern was observed in all cases, with PT1 overwhelmingly surpassing AAV2 in its ability to evade neutralization. However, some variation in neutralization scores (IVIG concentration for 50% neutralization) was observed, with a ratio of 3 between highest and lowest scores for AAV2 and 2.55 for PT1. Ratios between PT1 and AAV2 scores varied as well, from 4.9 in HuH-7 cells to 20.4 in ARPE-19 cells.

 doi:10.20944/preprints202409.2179.v

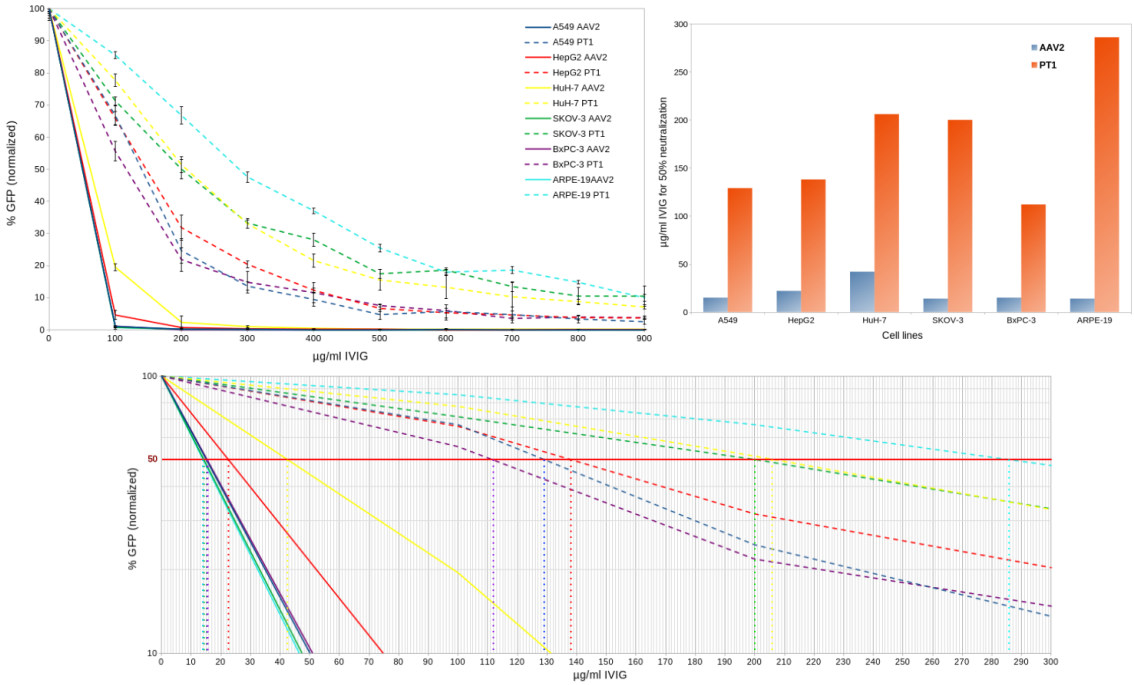

Figure 4. In vitro neutralization assays of PT1 and AAV2 capsids in 6 different cell lines. Top left: neutralization by IVIG of PT1 and AAV2 in 6 cell lines. Bottom: zoom on relevant area with Y-axis converted to logarithmic scale, showing IVIG concentrations at which transduction is decreased by 50%. Top right: comparison of neutralization scores between PT1 and AAV2 in 6 cell lines.

2.5. In Vivo Evaluation

Each of the 5 rAAV preparations was injected intravitreally into both eyes of 7 mice, 1 µl (7.22E9 vg) each. Eyes were harvested 3 weeks later. For each animal, one eye was processed into a flat mount in order to observe overall retinal transduction, while the other eye was processed as frozen sections to evaluate the biodistribution of GFP expression across the various retinal layers.

Retinal flat mount images are shown in Figure 5. AAV2 and its 2 derivatives quadYFTV and 7m8 showed the largest transduced areas, with 7m8 performing best. Very little GFP expression was observed with LSV1. While other variants showed mostly a continuous central area of GFP expression, in PT1 the expression was localized in smaller discrete areas distributed over the whole retina.

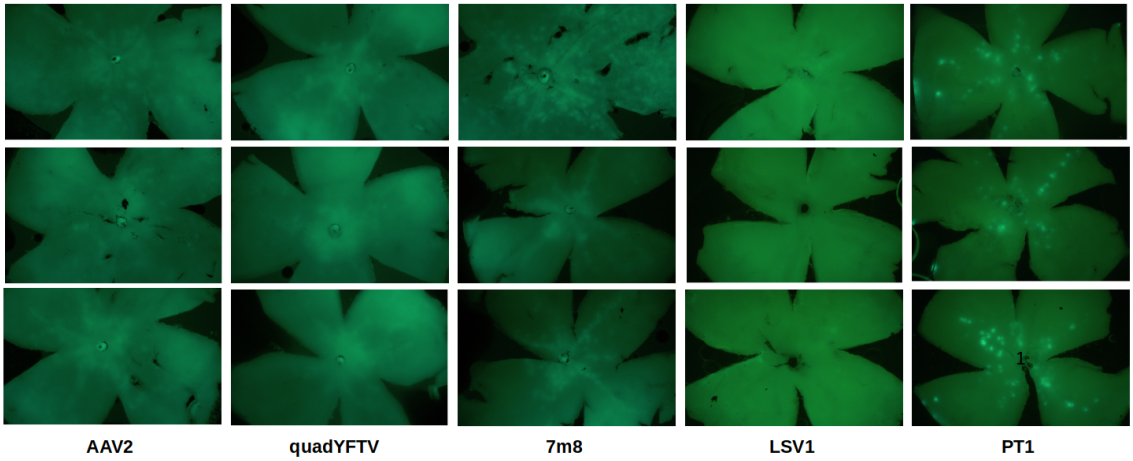

Figure 5. Retinal flat mounts. Fluorescence microscopy images of 3 representative retinal flat mounts are shown for each variant. From left to right: AAV2, quadYFTV, 7m8, LSV1, PT1. For LSV1 and PT1, exposure time was increased to make GFP expression more visible.

 doi:10.20944/preprints202409.2179.v

Retinal cryosections are shown in Figure 6. Again, the 3 AAV2-related capsid variants had broader transduction areas while LSV1 had the lowest transduction levels. PT1 was the only variant showing GFP expression in all retinal layers, including the outer nuclear layer (ONL) and beyond. In contrast, AAV2 and LSV1 had GFP expression restricted only to the ganglion cell layer (GCL) and inner nuclear layer (INL), while quadYFTV and 7m8 went slightly further up to the outer plexiform layer (OPL) right before the ONL. PT1 stands out with its unique ability to seemingly transduce all retinal layers and to penetrate much deeper than any of the control capsids.

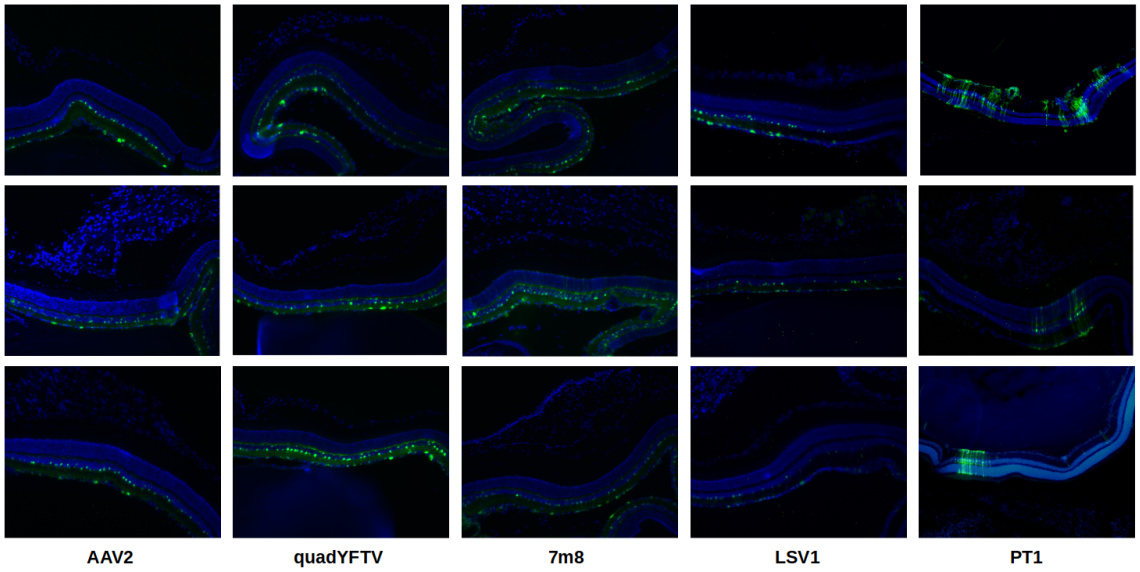

Figure 6. Retinal cryosections. Fluorescence microscopy images of 3 representative retinal cryosections are shown for each variant. From left to right: AAV2, quadYFTV, 7m8, LSV1, PT1.

3. Discussion

An AAV5-based multiple loop swap capsid library was developed and subjected to 2 rounds of in vivo selection in NHP. The AAV5 capsid was chosen as the library backbone because it had not yet been widely used for capsid libraries, it is the most divergent among human AAV capsid serotypes [16,17], it has excellent thermal stability [18] and it shows low prevalence of neutralizing antibodies among human populations [19]. The main purpose of the AAV5-derived capsid library was actually not to develop a retinal capsid, but rather to target organs such as liver, heart or kidneys through intravenous injection. It was decided to also inject intravitreally the same animals in order to maximize the amount of data that could be obtained per animal. It was a shot in the dark, as only AAV2-derived capsids were known to intravitreally transduce retina at the time, and there was low expectation that an AAV5-derived variant could do it as well. Nevertheless, an enriched variant was identified in retinal tissue, with a total of 8 amino acid substitutions in the 3 variable regions VR-III, VR-VI and VR-IX. As the VR-IV and VR-VIII regions were not mutated while they are the two regions with the highest spikes on the AAV5 capsid surface (see Figure 1), we decided to further evolve our variant by creating a capsid library based on it with mutations in those two regions, and subject the library to in vivo selection. Having no longer access to NHP, mice were used instead. After a single round of selection in retinal tissue after intravitreal injection, 7 additional amino acid substitutions were found to be strongly selected for, one in VR-IV and 6 in VR-VIII. The novel PT1 capsid variant combines the 15 mutations selected in NHP (8 mutations) and in mice (7 mutations) with an additional swap of the VP1 unique region with that of AAV8 to increase transduction efficiency (Figure 1). PT1 was compared to relevant capsid variants known to transduce retina after intravitreal injection, including AAV2 and 2 of its derivatives 7m8 and quadYFTV, as well as AAV5-derived LSV1.

 doi:10.20944/preprints202409.2179.v

Having a large number of mutations did not appear to interfere with capsid assembly, as production yield of PT1 was similar to that of LSV1 and higher than that of the AAV2-derived variants.

Ability to transduce retinal cells was first assessed in vitro using ARPE-19 cells, derived from human retinal pigmented epithelium. All 5 capsid variants showed similarly efficient transduction. When comparing transduction of various human-derived cell lines between PT1 and AAV2, PT1 showed a strong preference for the retinal cells ARPE-19, while AAV2 showed more versatility and a slight preference for liver-derived cells (Figure 2).

The most remarkable finding about PT1 is its striking ability to evade preexisting neutralizing antibodies (Figures 3 and 4). This is particularly relevant in the context of intravitreal delivery of gene therapies, as the vitreous is not as immune privileged as the subretinal space [4], and the availability of better immune-evading capsids will allow larger patient populations to be treated. This notable property of PT1 is not merely due to PT1 deriving from AAV5, since AAV5-derived LSV1 only performs slightly better than the 3 AAV2-derived capsids, far behind PT1. The number of surface mutations (15 and 9 for PT1 and LSV1 respectively) can not be the main reason either. An important difference between the two capsids is that all the 9 LSV1 mutations are confined within a very short 12 amino acid long region in VR-VIII, while the 15 PT1 mutations are spread over a huge, 331 amino acid long region and are present within 5 different variable regions (VR-III, VR-IV, VR-VI, VR-VIII and VR-IX), altering the capsid surface on a much larger scale. AAV5 capsid epitopes were previously described in structural studies involving 4 different monoclonal antibodies complexed with the AAV5 capsid [20–22]. Their overlap with LSV1 and PT1 mutations is shown in Table 1. Only 2 out of the 9 LSV1 mutations correspond to a contact position, both with the same antibody HL2476. On the other hand, 7 of the 15 PT1 mutations correspond to contact positions involving all 4 antibodies ADK5a (4 positions), ADK5b (3 positions), HL2476 (3 positions) and 3C5 (1 position). It should be noted that these 7 positions only represent a fraction of the footprints formed by the 4 reported antibodies. In particular, epitopes exist in regions VR-I, VR-II, VR-V, VR-VII and the HI loop which are all wild type in PT1, suggesting that even more radical immune evasion might be possible by introducing mutations in these regions. It remains to be seen, however, whether this could be achieved without compromising the efficiency of capsid assembly or the ability to transduce retinal cells.

Table 1. Mutated amino acid positions in LSV1 or PT1 that have previously been described as AAV5 epitopes. Numbers indicate amino acid position using AAV5 VP1 numbering (LSV1 and PT1 numbering are different because their VP1 unique regions were swapped with those of AAV2 and AAV8 respectively, which are of different length). ADK5a, ADK5b, HL2476 and 3C5 are monoclonal antibodies of which interactions with the AAV5 capsid were previously described. The plus sign indicates a contact position between the antibody and the capsid. Mutations in LSV1 and PT1 relative to AAV5 are shown (positions are wild type if blank).

Position	ADK5a [22]	ADK5b [22]	HL2476 [21]	3C5 [20]	LSV1	PT1
377	+					E to K
378	+					N to H
443		+	+			N to A
576			+			S to A
577			+		T to G	T to S
578			+		T to D	
697	+	+				Q to T
706	+	+		+		T to A

In vivo evaluation in mice showed that overall, 7m8 was the most effective at transducing retina, while PT1 was superior to LSV1 (Figures 5 and 6). However, while all controls transduced primarily the retinal layers closest to the vitreous (GCL and INL), PT1 showed much deeper penetration across the whole retina. It is unclear from the experimental data whether PT1 can transduce the retinal pigmented epithelium (RPE), an important therapeutic target. Additional experiments would be needed to

 doi:10.20944/preprints202409.2179.v

address this question. However, since LSV1 can supposedly transduce the RPE after intravitreal injection (which we could not observe due to unadequate experimental conditions), PT1 would be expected to show the same property, especially when considering its stronger ability to transduce all retinal layers. The most important limitation of this study is that the in vivo evaluation of PT1 was done in mice and not in the more clinically relevant NHP. However, 8 out of the 15 mutations of PT1 were actually selected in NHP. In addition, although in general capsid variants that perform well in rodents translate poorly when used in NHP or humans, it's less the case with retinal capsids. For example, 7m8 was selected in mice and has successfully been used in several clinical trials. Therefore, although NHP studies will be needed to further evaluate PT1's suitability as a human gene therapy capsid candidate, we have reasonable expectations regarding its potential, especially in view of its remarkable immune evasion properties.

4. Materials and Methods

4.1. AAV Capsid Libraries

Capsid libraries were designed and constructed as described previously [11,12]. The original library used in NHP was based on AAV5, while the library used in mice was based on a variant enriched from the original library. All libraries, including before and after enrichment, were analyzed using Illumina 2x150 paired-end sequencing.

4.2. AAV Preparations

Recombinant AAVs were prepared using triple plasmid transfection of adherent AAV-293 cells and purified by iodixanol gradient centrifugation as previously described [23]. The plasmid containing the GFP-encoding recombinant genome was pAAV-GFP [24]. When high endotoxin levels (>10 EU/ml) were detected, an additional endotoxin removal step [14] was performed.

4.3. AAV Quantification

Two µl AAV samples were first treated with Dnase I for 10 minutes at 37°C in a 20 µl volume. DNase was then inactivated by incubating at 75°C for 10 minutes in the presence of 25 mM EDTA. An equal volume of AAV lysis buffer (0.55 SDS, 20 mM Tris pH 8.0, 2 mM EDTA) was then added to each reaction, which was incubated at 70°C for 10 minutes. Samples were then further 50x diluted before being used as qPCR templates. The probe method was used to perform qPCR, with a linearized plasmid as the standard. Primers were ITR-F: 5'-GGAACCCCTAGTGATGGAGTT and ITR-R: 5'-CGGCCTCAGTGAGCGA. The probe was 5'-FAM and 3'-MGB labeled and its nucleotide sequence was 5'-CACTCCCTCTCTGCGCGCTCG.

4.4. In Vitro Transduction and Neutralization Assay

Wells of 96-well plates were seeded with 8E4 cells each. The next day, medium was aspirated before gently adding 50 µl of fresh culture medium containing 0 to 900 µg/ml IVIG (Sinopharm Wuhan Plasma-derived Biotherapies). After a 30 min incubation at 37°C, 50 µl of fresh culture medium containing one of the AAV capsid variant at MOI 10000 was added, before returning the plates to the incubator. Three replicates were made for each capsid variant / IVIG amount combination. Flow cytometry was performed 72 hours later. After removing medium, wells were washed with 40 µl PBS. After removing PBS, cells were detached from wells using 20 µl of Trypsin-EDTA. After complete detachment, cells were mixed with 150 µl of fresh medium before flow detection was performed on a Cytoflex S (Beckman Coulter).

4.5. Animals

For selection in NHP, 2 animals (Macaca fascicularis) were used in each of the 2 round, first male and female, then male only, weighting approximately 4 kg each. Selection in mice: 9 to 10 weeks old

 doi:10.20944/preprints202409.2179.v

male C57BL/6J mice were used. Capsid variant evaluation: 4 to 6 weeks old female C57BL6 mice were used.

4.6. Intravitreal rAAV Injections

Intravitreal injections of AAV capsid libraries into NHP were performed by Pharmalegacy (Shanghai). Two animals were used in each of the 2 rounds and injected into a single eye. In the first round, injection volume was 50 µl and capsid library titer was 1.44E13 vg/ml. In the second round, injection volume was 100 µl and capsid library titer was 6.07E13 vg/ml.

Intravitreal injections of AAV capsid library into mice were performed by SUSIMM (Suzhou) using 3 animals, with both eyes of each animal injected 5 µl of the AAV preparation which had a titer of 4.50E13 vg/ml.

The following describes intravitreal injections of rAAV preparations for capsid variant evaluation. Mice were anesthetized by intraperitoneal injection of 1.25% avertin (0.33-0.39 ml / 20 g animal weight). One microliter (7.22E9 vg) of rAAV particles was intravitreally injected using a 30 gauge beveled needle. The injection was performed free hand under a surgical microscope (66 Suzhou Vision-Tech). Both eyes were injected. Seven animals were used for each sample.

4.7. Retinal Harvesting

For capsid library selection in NHP, whole retinas were harvested by Pharmalegacy (Shanghai) 14 days after intravitreal injection.

For capsid library selection in mice, whole retinas were harvested by SUSIMM (Suzhou) 7 days after intravitreal injection.

For capsid variant evaluation, 3 weeks after intravitreal injection, mice were anesthetized by intraperitoneal injection of 1.25% avertin (0.33-0.39 ml / 20 g animal weight). Five minutes later, mice were euthanized by cervical dislocation. Eyes were enucleated by pulling apart the eyelids, placing a curved forceps under the eyeball, closing the forceps and gripping the connective tissue and optic nerve, being careful to avoid squeezing the eyeball, and gently pulling the eyeball from the orbit.

4.8. Retinal Flat Mounts

Eyes were fixed with 4% PFA (paraformaldehyde solution) at 4°C for 1 hour, then washed twice with PBS. An 18G needle was used to make a small hole in the posterior of the limbus. Micro-scissors were then used to cut around the circumference of the limbus. The cornea, iris, lens, and sclera were removed using forceps. The vitreous gel was extracted by gently squeezing it out with the help of micro-forceps. Two pairs of micro-forceps were used to go around the edges to separate the retina from the eyecup and then gently squeeze the retina out. The optic nerve head area was gently cut with micro forceps. The neuroretina was carefully peeled off the RPE/choroid and immersed in PBS buffer. Flat mounts were transferred to glass slides and mounted with the RGC layer facing upward using PBS. Images for assessment of GFP densities were acquired by fluorescence microscopy (Olympus IX70) and captured with a CCD camera (RETIGA 1300I) and associated software (Q Capture X64 software).

4.9. Retinal Cryosections

Enucleated eyes were fixed in 4% PFA/PBS for 4 h at 4°C followed by overnight incubation in 30% sucrose/PBS and embedded in optimal cutting temperature (OCT) reagent before being frozen. A Leica CM cryostat was used to make 15-20 µm sections, which were collected on slides coated with polylysine and stored at -20°C. Retinal sections were stained with DAPI solution (5 mg/L) for 10-15 minutes in the dark and washed twice with 0.1% Triton-X-100 in PBS. Slides were scanned and images were taken under an inverted fluorescence microscope (Olympus IX70).

4.10. Data Visualization

Protein sequence features were computed using Parent-map [25]. The three-dimensional capsid structure model was rendered by Pymol [26] using data (PDB ID 7KP3) obtained from VIPERdb [27].

 doi:10.20944/preprints202409.2179.v

4.11. Sequence Deposition

Nucleotide sequence of novel capsid variant PT1 was deposited in GenBank under accession number PQ252346.

5. Conclusions

The novel AAV capsid variant PT1 shows that AAV5 can be a suitable alternative to AAV2 as a parent capsid for evolving variants for retinal gene therapy via intravitreal injection, with advantages including higher production yield and a more favorable immune profile.

Incremental development, with selection of mutations in a limited set of variable regions followed by selection in another set of additional variable regions, combined with a rationally designed swap of the VP1 unique region, allowed the generation of a capsid variant with the desired property of improved retinal transduction after intravitreal injection without impairing the efficiency of capsid assembly.

Thanks to the large number of mutations spread over the capsid surface, with several positions overlapping with known epitopes, the novel capsid variant PT1 has a remarkable ability to evade preexisting neutralizing antibodies. This property makes PT1 a particularly promising candidate for human retinal gene therapy via intravitreal delivery, should future studies confirm its ability to efficiently transduce retina in clinically relevant animals.

6. Patents

A patent application for the PT1 engineered AAV capsid and its applications was filed by Porton Advanced Solutions under application number 2024107086717 with the China National Intellectual Property Administration.

Author Contributions: Conceptualization, D.M.; methodology, D.M.; software, D.M.; validation, Z.C., Y.L. and L.Z.; formal analysis, Z.C., Y.L. and L.Z.; investigation, Z.C., Y.L., L.Z, X.L., B.Z., Y.T., T.Z., Z.Z. and A.L.; resources, Q.J. and J.W.; data curation, Z.C., Y.L., L.Z. and D.M.; writing—original draft preparation, D.M.; writing—review and editing, Z.C., Y.L., J.W. and D.M.; visualization, Z.C. and D.M.; supervision, D.M. and D.L.; project administration, Z.C. and D.M.; funding acquisition, Q.J. and D.L. All authors have read and agreed to the published version of the manuscript.

Funding: D.L. was supported by National Key R&D Program 2023YFC2705602.

Institutional Review Board Statement: All animal experimental procedures were approved by the Institutional Animal Care and Use Committee (IACUC #20240111), ViewGene Biotech Co. Ltd (Suzhou, Jiangsu Province, China), and were carried out in accordance with the recommendations in the Guide for the Care and Use of Laboratory Animals, adhering to the ARVO Statement for the Use of Animals in Ophthalmic and Vision Research. The C57BL/6J male mice were purchased from Beijing Vital River Laboratory Animal Technology Co. Ltd, a branch of Charles River Laboratories.

Data Availability Statement: The original data presented in the study are openly available in FigShare at https://figshare.com/collections/PT1_AAV_capsid/7461079.

Acknowledgments: We would like to thank Lingjie Kong for his continuous support and exemplary leadership. We extend our deep gratitude to Oliver Ju who made this work possible thanks to his trust and generosity.

Conflicts of Interest: Z.C., L.Z., Y.L., Q.J. and D.M. are listed as inventors in the PT1 patent application.

Abbreviations

The following abbreviations are used in this manuscript:

VR	Variable region
GFP	Green fluorescent protein
vg	viral genome
rAAV	Recombinant AAV
NHP	Non-human primate
EDTA	Ethylenediaminetetraacetic acid
SDS	Sodium dodecyl sulfate
qPCR	Quantitative polymerase chain reaction
MOI	Multiplicity of infection

 doi:10.20944/preprints202409.2179.v

PBS	Phosphate-buffered saline
CCD	Charge-coupled device
PFA	Paraformaldehyde
DAPI	4′,6-diamidino-2-phenylindole

References

1. Wang, J.H.; Gessler, D.J.; Zhan, W.; Gallagher, T.L.; Gao, G. Adeno-associated virus as a delivery vector for gene therapy of human diseases. *Signal Transduction and Targeted Therapy* **2024**, *9*, 78. doi:10.1038/s41392-024-01780-w.
2. Liu, F.; Li, R.; Zhu, Z.; Yang, Y.; Lu, F. Current developments of gene therapy in human diseases. *MedComm* **2024**, *5*, e645. doi:10.1002/mco2.645.
3. Gao, J.; Hussain, R.M.; Weng, C.Y. Voretigene Neparvovec in Retinal Diseases: A Review of the Current Clinical Evidence. *Clinical Ophthalmology* **2020**, *Volume 14*, 3855–3869. doi:10.2147/OPTH.S231804.
4. Kotterman, M.A.; Yin, L.; Strazzeri, J.M.; Flannery, J.G.; Merigan, W.H.; Schaffer, D.V. Antibody neutralization poses a barrier to intravitreal adeno-associated viral vector gene delivery to non-human primates. *Gene Therapy* **2015**, *22*, 116–126. doi:10.1038/gt.2014.115.
5. Zolotukhin, S.; Vandenberghe, L. AAV capsid design: A Goldilocks challenge. *Trends in Molecular Medicine* **2022**, *28*, 183–193. doi:10.1016/j.molmed.2022.01.003.
6. Srivastava, A. Rationale and strategies for the development of safe and effective optimized AAV vectors for human gene therapy. *Molecular Therapy - Nucleic Acids* **2023**, *32*, 949–959. doi:10.1016/j.omtn.2023.05.014.
7. Dalkara, D.; Byrne, L.C.; Klimczak, R.R.; Visel, M.; Yin, L.; Merigan, W.H.; Flannery, J.G.; Schaffer, D.V. In Vivo–Directed Evolution of a New Adeno-Associated Virus for Therapeutic Outer Retinal Gene Delivery from the Vitreous. *Science Translational Medicine* **2013**, *5*. doi:10.1126/scitranslmed.3005708.
8. Pavlou, M.; Schön, C.; Occelli, L.M.; Rossi, A.; Meumann, N.; Boyd, R.F.; Bartoe, J.T.; Siedlecki, J.; Gerhardt, M.J.; Babutzka, S.; Bogedein, J.; Wagner, J.E.; Priglinger, S.G.; Biel, M.; Petersen-Jones, S.M.; Büning, H.; Michalakis, S. Novel AAV capsids for intravitreal gene therapy of photoreceptor disorders. *EMBO Molecular Medicine* **2021**, *13*, e13392. doi:10.15252/emmm.202013392.
9. Kellish, P.C.; Marsic, D.; Crosson, S.M.; Choudhury, S.; Scalabrino, M.L.; Strang, C.E.; Hill, J.; McCullough, K.T.; Peterson, J.J.; Fajardo, D.; Gupte, S.; Makal, V.; Kondratov, O.; Kondratova, L.; Iyer, S.; Witherspoon, C.D.; Gamlin, P.D.; Zolotukhin, S.; Boye, S.L.; Boye, S.E. Intravitreal injection of a rationally designed AAV capsid library in non-human primate identifies variants with enhanced retinal transduction and neutralizing antibody evasion. *Molecular Therapy* **2023**, *31*, 3441–3456. doi:10.1016/j.ymthe.2023.10.001.
10. Kay, C.N.; Ryals, R.C.; Aslanidi, G.V.; Min, S.H.; Ruan, Q.; Sun, J.; Dyka, F.M.; Kasuga, D.; Ayala, A.E.; Van Vliet, K.; Agbandje-McKenna, M.; Hauswirth, W.W.; Boye, S.L.; Boye, S.E. Targeting Photoreceptors via Intravitreal Delivery Using Novel, Capsid-Mutated AAV Vectors. *PLoS ONE* **2013**, *8*, e62097. doi:10.1371/journal.pone.0062097.
11. Marsic, D.; Govindasamy, L.; Currlin, S.; Markusic, D.M.; Tseng, Y.S.; Herzog, R.W.; Agbandje-McKenna, M.; Zolotukhin, S. Vector Design Tour de Force: Integrating Combinatorial and Rational Approaches to Derive Novel Adeno-associated Virus Variants. *Molecular Therapy* **2014**, *22*, 1900–1909. doi:10.1038/mt.2014.139.
12. Biswas, M.; Marsic, D.; Li, N.; Zou, C.; Gonzalez-Aseguinolaza, G.; Zolotukhin, I.; Kumar, S.R.; Rana, J.; Butterfield, J.S.; Kondratov, O.; De Jong, Y.P.; Herzog, R.W.; Zolotukhin, S. Engineering and In Vitro Selection of a Novel AAV3B Variant with High Hepatocyte Tropism and Reduced Seroreactivity. *Molecular Therapy - Methods & Clinical Development* **2020**, *19*, 347–361. doi:10.1016/j.omtm.2020.09.019.
13. Baker, C.K.; Bennett, A.; Belbellaa, B.; Nieves, J.; Tai, A.; NcKenna, R.; Cepeda, D.; Agbandje-McKenna, M.; Riley, B.E. Novel Capsid LSV1 Has a Unique 3D Structure at the Loop Substitution Area - Confers Superior Retinal Transduction from Intravitreal Injection. 2022 ASGCT Annual Meeting Abstracts. Molecular Therapy, 2022, Vol. 30, p. 575.
14. Kondratova, L.; Kondratov, O.; Ragheb, R.; Zolotukhin, S. Removal of Endotoxin from rAAV Samples Using a Simple Detergent-Based Protocol. *Molecular Therapy - Methods & Clinical Development* **2019**, *15*, 112–119. doi:10.1016/j.omtm.2019.08.013.
15. Dunn, K.; Aotaki-Keen, A.; Putkey, F.; Hjelmeland, L. ARPE-19, A Human Retinal Pigment Epithelial Cell Line with Differentiated Properties. *Experimental Eye Research* **1996**, *62*, 155–170. doi:10.1006/exer.1996.0020.

16. Chiorini, J.A.; Kim, F.; Yang, L.; Kotin, R.M. Cloning and Characterization of Adeno-Associated Virus Type 5. *Journal of Virology* **1999**, *73*, 1309–1319. doi:10.1128/JVI.73.2.1309-1319.1999.
17. Mietzsch, M.; Jose, A.; Chipman, P.; Bhattacharya, N.; Daneshparvar, N.; McKenna, R.; Agbandje-McKenna, M. Completion of the AAV Structural Atlas: Serotype Capsid Structures Reveals Clade-Specific Features. *Viruses* **2021**, *13*, 101. doi:10.3390/v13010101.
18. Bennett, A.; Patel, S.; Mietzsch, M.; Jose, A.; Lins-Austin, B.; Yu, J.C.; Bothner, B.; McKenna, R.; Agbandje-McKenna, M. Thermal Stability as a Determinant of AAV Serotype Identity. *Molecular Therapy - Methods & Clinical Development* **2017**, *6*, 171–182. doi:10.1016/j.omtm.2017.07.003.
19. Chhabra, A.; Bashirians, G.; Petropoulos, C.J.; Wrin, T.; Paliwal, Y.; Henstock, P.V.; Somanathan, S.; Da Fonseca Pereira, C.; Winburn, I.; Rasko, J.E. Global seroprevalence of neutralizing antibodies against adeno-associated virus serotypes used for human gene therapies. *Molecular Therapy - Methods & Clinical Development* **2024**, *32*, 101273. doi:10.1016/j.omtm.2024.101273.
20. Gurda, B.L.; DiMattia, M.A.; Miller, E.B.; Bennett, A.; McKenna, R.; Weichert, W.S.; Nelson, C.D.; Chen, W.j.; Muzyczka, N.; Olson, N.H.; Sinkovits, R.S.; Chiorini, J.A.; Zolotutkhin, S.; Kozyreva, O.G.; Samulski, R.J.; Baker, T.S.; Parrish, C.R.; Agbandje-McKenna, M. Capsid Antibodies to Different Adeno-Associated Virus Serotypes Bind Common Regions. *Journal of Virology* **2013**, *87*, 9111–9124. doi:10.1128/JVI.00622-13.
21. Jose, A.; Mietzsch, M.; Smith, J.K.; Kurian, J.; Chipman, P.; McKenna, R.; Chiorini, J.; Agbandje-McKenna, M. High-Resolution Structural Characterization of a New Adeno-associated Virus Serotype 5 Antibody Epitope toward Engineering Antibody-Resistant Recombinant Gene Delivery Vectors. *Journal of Virology* **2019**, *93*, e01394–18. doi:10.1128/JVI.01394-18.
22. Tseng, Y.S.; Gurda, B.L.; Chipman, P.; McKenna, R.; Afione, S.; Chiorini, J.A.; Muzyczka, N.; Olson, N.H.; Baker, T.S.; Kleinschmidt, J.; Agbandje-McKenna, M. Adeno-Associated Virus Serotype 1 (AAV1)- and AAV5-Antibody Complex Structures Reveal Evolutionary Commonalities in Parvovirus Antigenic Reactivity. *Journal of Virology* **2015**, *89*, 1794–1808. doi:10.1128/JVI.02710-14.
23. Crosson, S.M.; Dib, P.; Smith, J.K.; Zolotukhin, S. Helper-free Production of Laboratory Grade AAV and Purification by Iodixanol Density Gradient Centrifugation. *Molecular Therapy - Methods & Clinical Development* **2018**, *10*, 1–7. doi:10.1016/j.omtm.2018.05.001.
24. Gray, J.T.; Zolotukhin, S. Design and Construction of Functional AAV Vectors. In *Adeno-Associated Virus*; Snyder, R.O.; Moullier, P., Eds.; Humana Press: Totowa, NJ, 2012; Vol. 807, pp. 25–46. Series Title: Methods in Molecular Biology, doi:10.1007/978-1-61779-370-7_2.
25. Marsic, D. Parent-map: analysis of parental contributions to evolved or engineered protein or DNA sequences. *Journal of Open Source Software* **2021**, *6*, 2864. doi:10.21105/joss.02864.
26. Schrödinger, LLC. The PyMOL Molecular Graphics System, Version 3.0.
27. Montiel-Garcia, D.; Santoyo-Rivera, N.; Ho, P.; Carrillo-Tripp, M.; Iii, C.B.; Johnson, J.E.; Reddy, V.S. VIPERdb v3.0: a structure-based data analytics platform for viral capsids. *Nucleic Acids Research* **2021**, *49*, D809–D816. doi:10.1093/nar/gkaa1096.